

Different escape modes in two-photon double ionization of helium

A. S. Kheifets* and A. I. Ivanov

Research School of Physical Sciences, The Australian National University, Canberra ACT 0200, Australia

I. Bray†

ARC Centre for Matter-Antimatter Studies, Murdoch University, Perth, 6150 Australia

(Dated: October 15, 2018)

The quadrupole channel of two-photon double ionization of He exhibits two distinctly different modes of correlated motion of the photoelectron pair. The mode associated with the center-of-mass motion favors a large total momentum which is maximized at a parallel emission. However, the mode associated with the relative motion favors an antiparallel emission. This difference is manifested in a profoundly different width of the angular correlation functions corresponding to the center-of-mass and relative motion modes.

The process of correlated motion of multiple ionization fragments has been at the forefront of atomic collision physics during the past decade. Recent progress in experimental techniques made it possible to detect simultaneously a large number of charged reaction fragments with fully determined kinematics [1]. The long range Coulomb interaction between these fragments makes a full theoretical description of such a process a highly challenging task. In the meantime, the simplest multiple fragmentation reaction, the single-photon double ionization (SPDI) of helium is now well understood with accurate theoretical predictions being confirmed experimentally under a wide range of kinematical conditions [2, 3, 4]. All the information about the correlated motion of the photoelectrons is described in SPDI by a pair of symmetrized amplitudes $f^\pm(\theta_{12}, E_1, E_2)$ which depend on the relative interelectron angle and energy [5, 6]. If the photon is described by the linear polarization vector \hat{e} , the dipole matrix element of SPDI can be written simply as

$$D \propto f^+ (\hat{\mathbf{k}}_1 + \hat{\mathbf{k}}_2) \cdot \hat{e} + f^- (\hat{\mathbf{k}}_1 - \hat{\mathbf{k}}_2) \cdot \hat{e}, \quad (1)$$

where $\hat{\mathbf{k}}_i = \mathbf{k}_i/k_i$, $i = 1, 2$ are the unit vectors directed along the photoelectron momenta \mathbf{k}_i . Generalization of Eq. (1) to arbitrary polarization of light is straightforward [7]. Under the equal energy sharing condition, the anti-symmetric amplitude vanishes $f^-(E_1 = E_2) = 0$ and all the information about the SPDI process is contained in one symmetric amplitude f^+ . Following predictions of the Wannier-type theories [8, 9], the SDPI amplitude can be written using the Gaussian ansatz:

$$|f^+|^2 \propto \exp \left[-4 \ln 2 \frac{(\pi - \theta_{12})^2}{\Delta \theta_{12}^2} \right] \quad (2)$$

where the width parameter $\Delta \theta_{12}$ indicates the strength of angular correlation in the two-electron continuum. Although the analytical theories [8, 9] validate Eq. (2) only near the double ionization threshold, numerical models

[10] and direct measurements [11, 12] support its validity in a far wider photon energy range [10].

Two-photon double ionization (TPDI) of He is a much more complex fragmentation process with two competing decay channels into the S and D two-electron continua. In a most general case, complete separation of the dynamic and kinematical variables in TPDI requires introduction of five symmetrized amplitudes [13] or four unsymmetrized amplitudes [14].

In this Letter, we demonstrate that complexity of the TPDI leads to a new phenomenon of two distinct correlated escape modes: one is associated with the center-of-mass motion of the photoelectron pair whereas another is related to their relative motion. The center-of-mass motion favors a large total momentum of the pair $\mathbf{p} = \mathbf{k}_1 + \mathbf{k}_2$ which is gained at a parallel escape. In this configuration, the inter-electron repulsion is strongest and the angular correlation factor has a relatively narrow width. On the contrary, the relative motion favors a large relative momentum $\mathbf{k} = \mathbf{k}_1 - \mathbf{k}_2$ which is maximized at an antiparallel escape. In this configuration, the inter-electron repulsion is weak. This results in a profoundly large angular correlation width as compared with the center-of-mass motion.

For simplicity, we consider equal-energy-sharing kinematics $E_1 = E_2$ and restrict ourselves with only the dominant quadrupole TPDI amplitude. By performing a derivation similar to Ref. [13], the quadrupole amplitude can be parametrized as

$$Q \propto \left[g_k \{ \hat{\mathbf{k}} \otimes \hat{\mathbf{k}} \}_2 + g_p \{ \hat{\mathbf{p}} \otimes \hat{\mathbf{p}} \}_2 + g_0 \left\{ [\hat{\mathbf{k}} \times \hat{\mathbf{p}}] \otimes [\hat{\mathbf{k}} \times \hat{\mathbf{p}}] \right\}_2 \right] \cdot \{ \hat{e} \otimes \hat{e} \}_2 \quad (3)$$

Here we introduced the unit vectors $\hat{\mathbf{p}} = \mathbf{p}/p$ and $\hat{\mathbf{k}} = \mathbf{k}/k$. The symmetrized amplitudes in Eq. (3) are defined as

$$g_{k,p}(x) = \sum_{l=0} \frac{1}{2} D_l [P_l''(x) + P_{l+2}''(x) \pm 2P_{l+1}''(x)] Q_{l+2}(k_1, k_2) \mp \frac{1}{4} C_l P_l''(x) Q_{ll}(k_1, k_2), \quad (4)$$

*Electronic address: A.Kheifets@anu.edu.au

†Electronic address: I.Bray@murdoch.edu.au

$$g_0(x) = \sum_{l=2} C_l P_l''(x) Q_{ll}(k_1, k_2).$$

Here the upper and lower sets of signs refers to g_k and g_p , respectively. These amplitudes depend on the interelectron angle $x = \cos \theta_{12}$ and are expressed via the quadrupole radial matrix elements $Q_{ll'}(k_1, k_2)$ and the Legendre polynomial derivatives $P_l''(x)$. Normalization coefficients C_l and D_l are given in Ref. [15]. Using similar notations, the dipole amplitude of SPDI (1) under the equal energy sharing condition is parametrized as $D \propto f_p (\hat{\mathbf{p}} \cdot \hat{\mathbf{e}})$, $f^+ \equiv f_p$, $f^- = 0$. We note that D is *linear* with respect to $\hat{\mathbf{p}}$ and does not contain $\hat{\mathbf{k}}$ under the equal energy condition. In contrast, Q is *quadratic* with respect to $\hat{\mathbf{k}}$ and $\hat{\mathbf{p}}$ and contains both vectors even when $E_1 = E_2$. The amplitude g_k which enters Eq. (3) with the tensorial product $\{\hat{\mathbf{k}} \otimes \hat{\mathbf{k}}\}_2$ can be associated with the relative motion of the photoelectron pair described by the vector \mathbf{k} . Similarly, the amplitudes g_p can be associated with the center-of-mass motion and the amplitude g_0 which is entering Eq. (3) with the vector product $\hat{\mathbf{k}} \times \hat{\mathbf{p}}$ can be associated with the mixed motion mode.

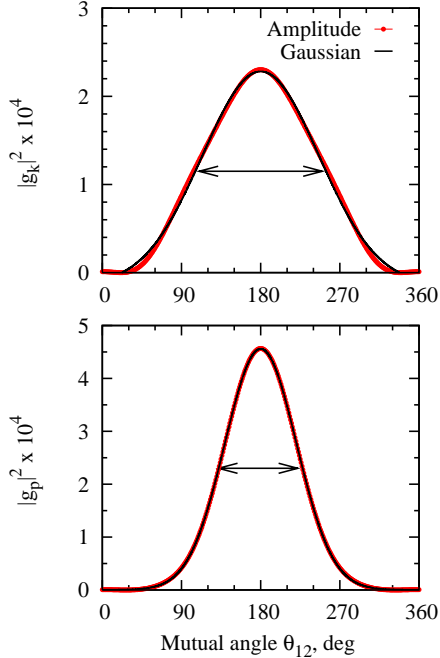


FIG. 1: The TPD amplitudes in the quadrupole channel g_k (top) and g_p (bottom) fitted with the Gaussian ansatz (2). The excess energy of 4 eV is shared equally between the photoelectrons $E_1 = E_2 = 2$ eV. The arrows indicate the Gaussian width parameter $\Delta\theta_{12}$.

To calculate the radial matrix elements $Q_{ll'}(k_1, k_2)$, we employed here the same dynamical model as was outlined in our previous work [13]. In this model, the electron-photon interaction was treated in the lowest-order perturbation theory using the closure approximation whereas the electron-electron interaction was included in full using the convergent close-coupling (CCC)

method. The model proved to be capable of describing the angular correlation pattern in the two-electron continuum in good agreement with non-perturbative, with respect to the electromagnetic interaction, calculations [16, 17].

We calculated amplitudes (4) in a range of excess energies $E_1 + E_2$ from 1 eV to 20 eV above the double ionization threshold. We employed a fairly large CCC basis set composed typically of 25 – l box-space target states [18] with $0 \leq l \leq 6$. Convergence of the calculation with respect to the basis size was thoroughly tested.

In the whole excess energy range, the amplitude g_0 was found insignificant as compared with g_k and g_p . The latter amplitudes were fitted with the Gaussian ansatz (2). A typical quality of the fit can be judged from Figure 1 where the amplitudes g_k and g_p are exhibited for $E_1 = E_2 = 2$ eV. The corresponding width parameters $\Delta\theta_{12}$ are plotted in Figure 2, as a function of energy, along with the width parameter of the dipole amplitude f_p .

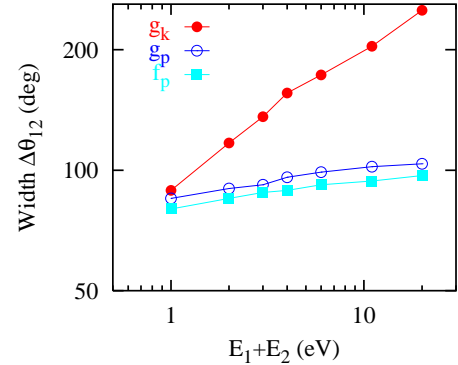


FIG. 2: The Gaussian width parameters $\Delta\theta_{12}$ of the amplitudes g_k (red filled circles), g_p (blue open circles) and f_p (light blue squares) as functions of the excess energy $E_1 + E_2$. Extraction of the width parameters is illustrated in Figure 1 for $E_1 = E_2 = 2$ eV.

We observe a much larger Gaussian width of the relative motion amplitude g_k as compared with the center-of-mass motion amplitudes g_p and f_p , the latter two having a very similar width. We interpret this stark difference in terms of the strength of the electron-electron repulsion. This strength is much larger in the center-of-mass motion which favors large p and hence parallel emission, as opposed to the relative motion which favors large k associated with anti-parallel emission. We note that the mixed mode amplitude is typically an order of magnitude smaller than the pure mode amplitudes g_k and g_p thus supporting our notion of distinct escape modes.

In the case of co-planar geometry when all three vectors \mathbf{k}_1 , \mathbf{k}_2 and $\hat{\mathbf{e}}$ belong to the same plane, we can choose the coordinate frame as $z \parallel \mathbf{k}_1$ and $x \parallel [\mathbf{k}_1 \times \mathbf{k}_2]$. In this case, Eq. (1) and Eq. (3) are simplified to

$$D \propto f_p (\cos \theta_1 + \cos \theta_2) \quad (5)$$

$$\begin{aligned}
Q \propto & g_k \left[(\cos \theta_1 - \cos \theta_2)^2 - \frac{2}{3}(1 - \cos \theta_{12}) \right] \\
& + g_p \left[(\cos \theta_1 + \cos \theta_2)^2 - \frac{2}{3}(1 + \cos \theta_{12}) \right] \\
& + \frac{1}{3}g_0(\cos^2 \theta_{12} - 1)
\end{aligned} \quad (6)$$

From these equations, it is seen that the amplitudes f_p and g_p related to the center-of-mass mode, and the amplitude g_k related to the relative motion mode, contribute quite differently to the corresponding matrix elements. All three amplitudes peak strongly near $\theta_{12} = 180^\circ$. However, the kinematic factors corresponding to f_p and g_p have nodes at this angle whereas the kinematic factor accompanying g_k has a peak. As a result, the term proportional to g_k dominates strongly the quadrupole amplitude. This dominance is illustrated in Figure 3 where the triply-differential cross-section $d\sigma/dE_1 d\Omega_1 d\Omega_2 \propto |Q|^2$ of the TPDI of He at $E_1 = E_2 = 2$ eV and the coplanar kinematics is plotted as a function of the variable escape angle θ_2 . Various panels from top to bottom correspond to fixed escape angles $\theta_1 = 0^\circ, 30^\circ, 60^\circ$ and 90° . Two calculations are displayed in the figure: one with the full quadrupole amplitude Eq. (6) and another with only the g_k contribution. The dominance of the g_k term is evident at all fixed angles θ_2 . It is particularly strong at a fix escape angle $\theta_1 = 0$ when nearly all the contribution to the quadrupole amplitude comes from the g_k term.

We note that in our previous paper [13] we introduced a slightly different set of amplitudes in the quadrupole channel:

$$\begin{aligned}
Q \propto & \frac{2}{3} \left\{ g^+ \left[P_2(\cos \theta_1) + P_2(\cos \theta_2) \right] \right. \\
& \frac{1}{2} g_s \left[3 \cos \theta_1 \cos \theta_2 - \cos \theta_{12} \right] \\
& \left. \frac{1}{2} g_0 (\cos^2 \theta_{12} - 1) \right\}
\end{aligned} \quad (7)$$

where

$$\begin{aligned}
g^+ &= g_p + g_k \\
g_s &= 2(g_p - g_k)
\end{aligned} \quad (8)$$

Although the set of amplitudes (8) gives an identical quadrupole amplitude, it does not provide such a clear separation of the center-of-mass and relative motion modes. Our earlier attempt in Ref. [13] to apply the Gaussian ansatz (2) showed no such a clear systematic behavior of the angular correlation width with respect of the excess energy as exhibited in Figure 2.

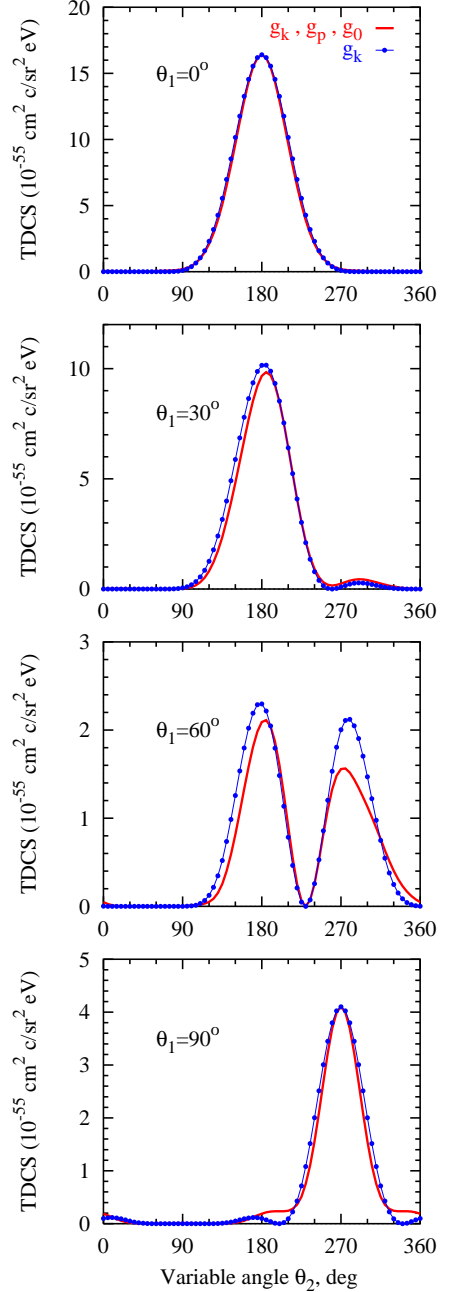


FIG. 3: Triply-differential cross-section $d\sigma/dE_1 d\Omega_1 d\Omega_2 \propto |Q|^2$ of the TPDI of He at $E_1 = E_2 = 2$ eV in the coplanar kinematics is plotted as a function of the variable escape angle θ_2 . Various panels from top to bottom correspond to fixed escape angles $\theta_1 = 0^\circ, 30^\circ, 60^\circ$ and 90° . The red solid line corresponds to the full quadrupole amplitude (6) whereas the blue dotted line exhibits the contribution of the g_k term only.

In conclusion, we demonstrated the presense of the two distinct photoelectron escape modes following two-photon double ionization of He. One of the modes corresponds to the center-of-mass motion of the photoelectron pair. It enhances the total momentum of the pair and therefore favors the parallel emission. The inter-electron repulsion is strong in this mode and the angular correlation width is relatively small. The other, relative motion, mode enhances the relative momentum of the pair and therefore favors the antiparallel emission. The inter-electron repulsion is much weaker in this mode and the angular correlation width is much larger. Both modes are fully symmetric and present under the equal energy sharing condition. In contrast, the single-photon double ionization has only one fully symmetric mode which is

associated with the center-of-mass motion. This mode, in terms of the angular correlation width, is very similar to the center-of-mass motion mode in two-photon double ionization. The presense of two modes is simply a reflection of the quadratic tensorial structure of the quadrupole photoionization amplitude as compared to the linear structure of the dipole photoionization amplitude.

The authors wish to thank Australian Partnership for Advanced Computing (APAC) and ISA Technologies, Perth, Western Australia, for provision of their computing facilities. Support of the Australian Research Council in the form of Discovery grant DP0451211 is acknowledged.

-
- [1] J. Ullrich *et al.*, Rep. Prog. Phys. **66**, 1463 (2003).
 - [2] J. S. Briggs and V. Schmidt, J. Phys. B **33**, R1 (2000).
 - [3] G. C. King and L. Avaldi, J. Phys. B **33**, R215 (2000).
 - [4] L. Avaldi and A. Huetz, J. Phys. B **38**, S861 (2005).
 - [5] A. Huetz, P. Selles, D. Waymel, and J. Mazeau, J. Phys. B **24**, 1917 (1991).
 - [6] L. Malegat, P. Selles, and A. Huetz, J. Phys. B **30**, 251 (1997).
 - [7] S. J. Schaphorst *et al.*, J. Electron Spectrosc. Relat. Phenom. **76**, 229 (1995).
 - [8] A. R. P. Rau, J. Phys. B **9**, L283 (1976).
 - [9] J. M. Feagin, J. Phys. B **17**, 2433 (1984).
 - [10] A. S. Kheifets and I. Bray, Phys. Rev. A **65**, 022708 (2002).
 - [11] P. Bolognesi *et al.*, J. Phys. B **36**, L241 (2003).
 - [12] A. Knapp *et al.*, J. Phys. B **28**, 645 (2005).
 - [13] A. S. Kheifets and I. A. Ivanov, J. Phys. B **39**, 1731 (2006).
 - [14] E. A. Pronin *et al.*, *37th Meeting of the Division of Atomic, Molecular and Optical Physics* (American Physical Society, Knoxville, TN, 2006).
 - [15] N. L. Manakov, S. I. Marmo, and A. V. Meremianin, J. Phys. B **29**, 2711 (1996).
 - [16] J. Colgan and M. S. Pindzola, Phys. Rev. Lett. **88**, 173002 (2002).
 - [17] S. X. Hu, J. Colgan, and L. A. Collins, J. Phys. B **38**, L35 (2005).
 - [18] I. Bray, K. Bartschat, and A. T. Stelbovics, Phys. Rev. A **67**, 060704(R) (2003).